J. Fluid Mech. (2010), *vol.* 643, *pp.* 425–435. © Cambridge University Press 2010
doi:10.1017/S0022112009992680

Horizontal mixing of quasi-uniform straight compound channel flows

ALESSANDRO STOCCHINO[1]† AND MAURIZIO BROCCHINI[2]

[1]Dipartimento di Ingegneria delle Costruzioni, dell'Ambiente e del Territorio, University of Genova, Via Montallegro 1, 16145 Genova, Italy

[2]Department of I.S.A.C., Polytechnic University of Marche, Via Brecce Bianche 12, 60131 Ancona, Italy

(Received 28 July 2009; revised 9 October 2009; accepted 9 October 2009)

The generation and evolution of large-scale vortices with vertical axis (macro-vortices) in a straight compound channel under quasi-uniform flow conditions is investigated. We discuss possible similarities and clear differences with free shear layer flows induced by the meeting of shallow streams of different speeds. An experimental investigation based on particle image velocimetry (PIV) measurements of free-surface velocities forms the basis for an analysis of both the specific features of macro-vortices and of the related mean flow characteristics. Dynamical properties strongly depend on the ratio r_h between the main channel flow depth (h^*_{mc}) and the floodplain depth (h^*_{fp}), and three flow classes can be identified. 'Shallow flows' ($r_h > 3$) are dominated by strong shearing and large macro-vortices populating the transition region between the main channel and the floodplains. The mean streamwise velocity induced in 'intermediate flows' ($2 \leqslant r_h \leqslant 3$) is characterized by a dip in the transition region, while it closely resembles that occurring in a rectangular channel in the case of 'deep flows' ($r_h < 2$). For both the latter cases the shear in the transition region decreases and the macro-vortices are also generated in the wall boundary layer of the floodplains. The typical size of the quasi-two-dimensional macro-vortices, generated at the transition region, is found to be independent of the streamwise coordinate. This and the non-monotonic behaviour of the mean streamwise velocity suggest that in straight compound channels the topographic forcing is so dominant that conceptual models interpreting these flows as free shear layers may largely fail to describe the physics of compound channels flows.

Key words: compound channel, macro-vortices, mixing, shallow flow, shear layer

1. Introduction

A great variety of natural water streams and artificial channels can be classified as 'compound channels' since their cross-stream section can be assumed to be characterized by a main channel and shallow floodplains. Flows of these streams are defined as predominantly horizontal since their horizontal dimensions greatly exceed the vertical one (Jirka 2001; van Prooijen & Uijttewaal 2002). Although in bounded shear flows the three-dimensional turbulent eddy size is, typically, limited to the shortest dimension (in this case, the water depth), large-scale two-dimensional coherent structures with length scales greater than the water depth are observed in a wide range of shallow shear flows (Jirka 2001; Socolofksy & Jirka 2004). Among

† Email address for correspondence: jorma@dicat.unige.it

studies on the evolution of quasi-two-dimensional vortices with vertical axes (macro-vortices) in compound channels important are those of Sellin (1964), Shiono & Knight (1991) and Nezu, Onitsuka & Iketani (1999). The different mechanisms that may lead to the production of vorticity in shallow streams and, ultimately, macro-vortices have been recently described by Jirka (2001) and Nikora *et al.* (2007). Among them, the topographic forcing that imposes an abrupt gradient in the flow evolution has been recognized as the main agent for the generation of macro-vortices. In the same vein Soldini *et al.* (2004), using the classic shallow-water approach, have illustrated the mechanism by which depth discontinuities at the transition between the main channel and the floodplains (either 'transition' or 'transition region' in the following) are able to produce potential vorticity and, thus, sustain the generation of macro-vortices. These turbulent structures are recognized to be responsible for the transfer of momentum and mass from the main channel to the floodplains. As a consequence, the velocity decreases in the main channel and increases in the floodplains, possibly resulting in a modified conveyance capacity (van Prooijen, Battjes & Uijttewaal 2005).

In many applications of river engineering and river training works a compound geometry is purposely created and, therefore, the estimate of the water discharge, velocity and Reynolds stresses profiles and the prediction of the overbank front speed during short duration floods is clearly important (Shiono & Knight 1991; van Prooijen *et al.* 2005). Moreover, floodplains in natural river are often wetlands with abundant wild life and the knowledge of the mass transport processes is vital to preserve the environmental conditions. In this respect, the large-scale macro-vortices play a fundamental role on the transverse exchange of mass (e.g. pollutants, nutrients) between the main channel and the floodplains (van Prooijen & Uijttewaal 2002).

However, until recently very simple conceptual models have been used to represent the mentioned lateral mixing which has been mainly accounted for through an empirical apparent shear stress (e.g. Stephenson & Kolovopoulos 1990). Such a perspective, only adequate for steady-state conditions and based on an integral model, is being replaced by an approach for which the major agents of transport of mass and momentum are the discrete flow structures above defined as macro-vortices. A common theoretical approach used to describe uniform compound channel flows relies on the apparent close similarity between the flow at the 'transition' and the flow generated at the interfaces of two free shallow streams with different velocities. Such a similarity is based on the evidence that for both these configurations it is possible to use the same sort of stability analysis and also that mean velocity profiles can be, in both cases, well described by bell-shaped functions (e.g. hyperbolic tangent/secant).

The present contribution focuses on the description of the dynamics undergone by macro-vortices in a compound channel as part of the overall flow evolution. More specifically, we intend to clarify the validity and ambiguities concerned with the representation of the flow at the transition in a straight compound channel as a free shear layer flow. Since secondary circulations are shown to be of minor importance in straight uniform compound channel flows (van Prooijen & Uijttewaal 2002; van Prooijen *et al.* 2005), the experimental analysis which forms the basis of our study is only concerned with the description of horizontal (at the surface) flow features.

2. Experimental set-up and data analysis

Physical experiments have been carried out at the laboratory of the Department of Civil, Environmental and Architectural Engineering of the University of Genova using a flume that is 20 m long, 60 cm wide and whose trapezoidal cross-section is composed

Experiment Name	r_h (—)	Q^* ($\mathrm{l\,s^{-1}}$)	U_m^* ($\mathrm{cm\,s^{-1}}$)	$Re \times 10^4$	Fr (—)
Shallow flows					
Q008	6.0	3.3	37.4	1.3	0.48
Q012	5.7	4.1	37.5	1.4	0.49
Q018	4.0	5.0	40.0	1.6	0.50
Q027	3.5	6.1	42.7	1.7	0.52
Intermediate flows					
Q056	2.7	8.8	46.4	2.1	0.53
Q120	2.3	12.9	56.3	2.7	0.60
Q180	2.1	15.7	60.7	3.0	0.63
Deep flows					
Q287	1.9	19.9	65.0	3.4	0.64
Q350	1.8	22.0	68.0	3.6	0.66

TABLE 1. Hydraulic conditions at $x^* = 7\,\mathrm{m}$.

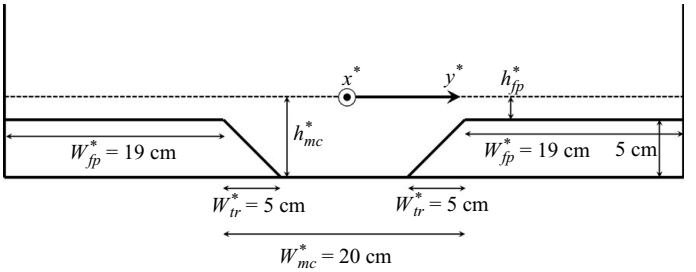

FIGURE 1. Sketch of the cross-section of the flume.

by a central main channel ($W_{mc}^* = 20$ cm), two lateral flat floodplains ($W_{fp}^* = 19$ cm) and a transition region ($W_{tr}^* = 5$ cm) (see figure 1). We use a Cartesian coordinate system in which x^* and y^* are aligned with the streamwise and spanwise direction of the flow, respectively (see also figure 1). In the following, horizontal distances are normalized by the main channel half-width ($W_{mc,hw}^* = 10$ cm). The compound channel, including the lateral vertical walls, is made of sheets of polyvinyl chloride (PVC) 1 cm thick. Three measuring sections have been selected in the longitudinal direction placed at 2, 5 and 7 m downstream of the flume inlet. Hydraulic conditions of the experiments, referring to the most downstream section, can be found in table 1, where $r_h = h_{mc}^*/h_{fp}^*$ is the ratio between the main channel water depth and that of the floodplains, Q^* is the discharge and U_m^* the peak velocity in the main channel. $Re = (R^* U_m^*)/\nu$ is the Reynolds number and $Fr = U_m^*/\sqrt{gR^*}$ is the Froude number, where R^* is the hydraulic radius. The most downstream section, $x^* = 7$m, is characterized by fully established flow conditions both in terms of bottom boundary layer and transition shear layer evolution. According to Bousmar *et al.* (2005) compound channel flows are fully established at a length L^* downstream of the inception with $L^*/W_{fp}^* > 35$. In the present case the length L^* is greater than 6.6 m. Measurements of two-dimensional velocity fields on the free surface have been obtained by means of a two-dimensional PIV analysis using the IDT software package. An high-speed digital camera has been used to record 2000 frames for each acquisition, with acquisition frequency between 100 and 200 Hz. The illumination has been provided by three white light incandescent lamps of 1000 W each and white plastic particles with a

mean diameter of 300 μm and a specific gravity of about 1.05 were used as tracers for the PIV. We have preventively treated the particles with ethyl alcohol to avoid clustering on the free surface. This gave an approximate area density of about 10 particle cm^{-2}. The area of interest for the flow measurements has dimensions of about $(0.6 \times 0.6)m^2$ and (1024×1024)pixel. Probability density functions (PDFs) of the measured displacements have been calculated to verify the occurrence of peak-locking effect. The shape of the PDFs, being almost Gaussian, suggests that the measured velocity are not affected by this error. The flow depth has been monitored along the streamwise direction during each experiment and the differences detected among the measuring sections was less than the 1 %.

The resulting two-dimensional velocity vectors have been elaborated to extract the main features of the flow under investigation. A specific analysis to identify and to track vortical structures has also been carried out. Among the many techniques of vortex identification, we employed the method based on the evaluation of the swirling strength λ_{ci}, commonly used in turbulence measurements to study coherent structures (Adrian, Christensen & Liu 2000). The swirling strength, defined as the positive imaginary eigenvalue of the local velocity gradients tensor, is large where there is a strong rotation of the flow, i.e. a vortex. Moreover, to help the visualization of the macro-vortices embedded in the flow we have introduced a Galilean decomposition removing from the actual flow field a constant longitudinal advection velocity, chosen as the areal-averaged streamwise velocity, as suggested in Adrian *et al.* (2000). If the constant velocity removed matches the convective velocity of the vortices, the latter appears as an almost circular pattern of vectors plotting the residual part of the velocities. The resulting contour maps of λ_{ci} have been used to study the main geometrical features and the evolution of the vortical structures, after having applied a threshold of about 5 % of the maximum value to remove the background noise. In particular, we could infer the position of the core of the vortex, the radius of the area-equivalent circle R^*_{eq}, and other geometrical characteristics of interest, e.g. the eccentricity ϵ of the vortices and the inclination angle θ with respect to the mean flow. The equivalent radius has been normalized (R_{eq}) using as a characteristic length scale the width of the transition region (W^*_{tr}), where the flow experiences the depth jump. Normalized PDFs of the above features have been obtained. The total number of vortices revealed during a single experiment ranges between 200 and 400.

3. Experimental observations

The main experimental results are concerned with both the mean quantities (streamwise velocity and Reynolds stress) and the macro-vortices. In particular, the data presented in the rest of this section regards the most downstream measuring section, $x = 70$.

3.1. *The mean flow*

The two-dimensional velocity vector outputs of the PIV analysis have been elaborated to extract the main flow features. In particular, we have performed an ensemble average on the velocity fields and, then, spatial averages along the streamwise direction to extract dimensionless mean streamwise velocity (u) profiles and profiles of dimensionless averaged Reynolds stress ($\overline{u'v'}$). The velocity scale used to normalize the above quantities is the velocity at the transition ($y = 1$). In the following, results are analysed with the reference to the classification introduced by Nezu *et al.* (1999).

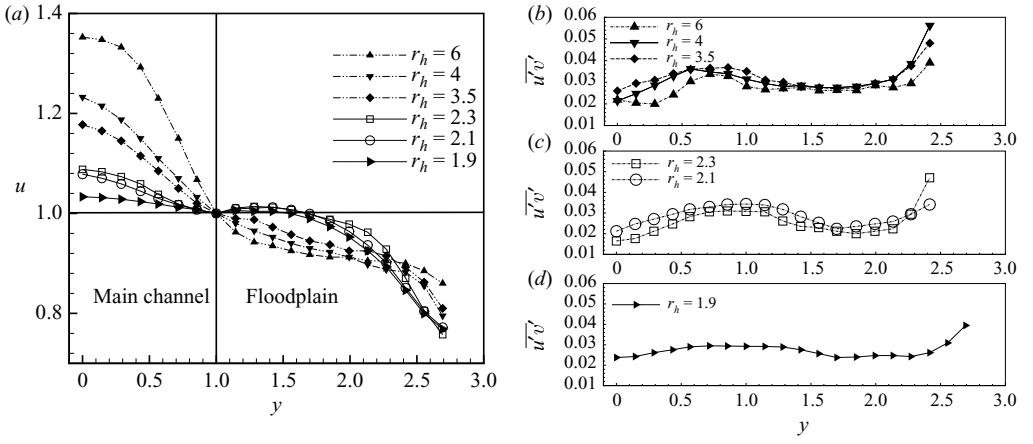

FIGURE 2. Mean streamwise surface velocity (*a*) and averaged Reynolds stress (*b–d*) for different values of r_h.

(*a*) The 'shallow flows' ($r_h > 3$) are characterized by monotonic velocity profiles and a strong velocity gradient at the transition between the main channel and the floodplain (see figure 2*a*). In fact, the ratio between the peak main channel velocity ($y = 0$) and the floodplain velocity ($y = 1$) is of order 1.3–1.5. This leads to a strong shearing in the transition and is associated with intense macro-vortices. At the wall boundary layers only a weak shear occurs and almost no macro-vortices are generated. The spanwise profile of $\overline{u'v'}$ (figure 2*b*) presents a local maximum at $y = 1$ where the flow jump intensifies the generation of turbulence. This feature is found also for the next class of flows (see figure 2*c*).

(*b*) The 'intermediate flows' ($2 < r_h < 3$) are characterized by non-monotonic velocity profiles with a dip over the transition (see figure 2*a*). According to Nezu *et al.* (1999) this effect is the signature of counter-rotating macro-vortices at the transition (see also figure 3*c*). The ratio between the peak main channel velocity and the floodplain velocity is 1.05–1.15 and, thus, weaker than for the 'shallow flows'. The depth increase leads to a growth of the wall boundary layer thickness and macro-vortices are generated, by wall-adherence-induced shearing, also in the floodplain close to the walls, as we discuss in the next section.

(*c*) The 'deep flows' ($r_h < 2$) are characterized by a very weak shear in the transition region, but there is still influence of the compound channel geometry on the surface velocity profiles (see figure 2*a*). The ratio between the peak main channel velocity and the floodplain velocity is 1.00–1.05. The wall boundary layer increases in size and more and stronger macro-vortices are generated over the floodplains. However, the influence of the topography is much weaker and this can also be seen in the distribution of $\overline{u'v'}$ that is flatter except close to the lateral wall (figure 2*d*).

3.2. *The macro-vortices*

In order to better understand the overall flow field and characteristics of macro-vortices, instantaneous measurements of the surface flow velocity are analysed by means of vortex identification and vorticity fields, Galilean decomposition of the velocity field and Power spectral density (PSD) distributions of point-like velocity signals. Generation of two-dimensional macro-vortices has been observed for all the values of r_h investigated. The classification of the flow regimes used to characterize the mean velocity profile can be applied also when the free surface vortical structures

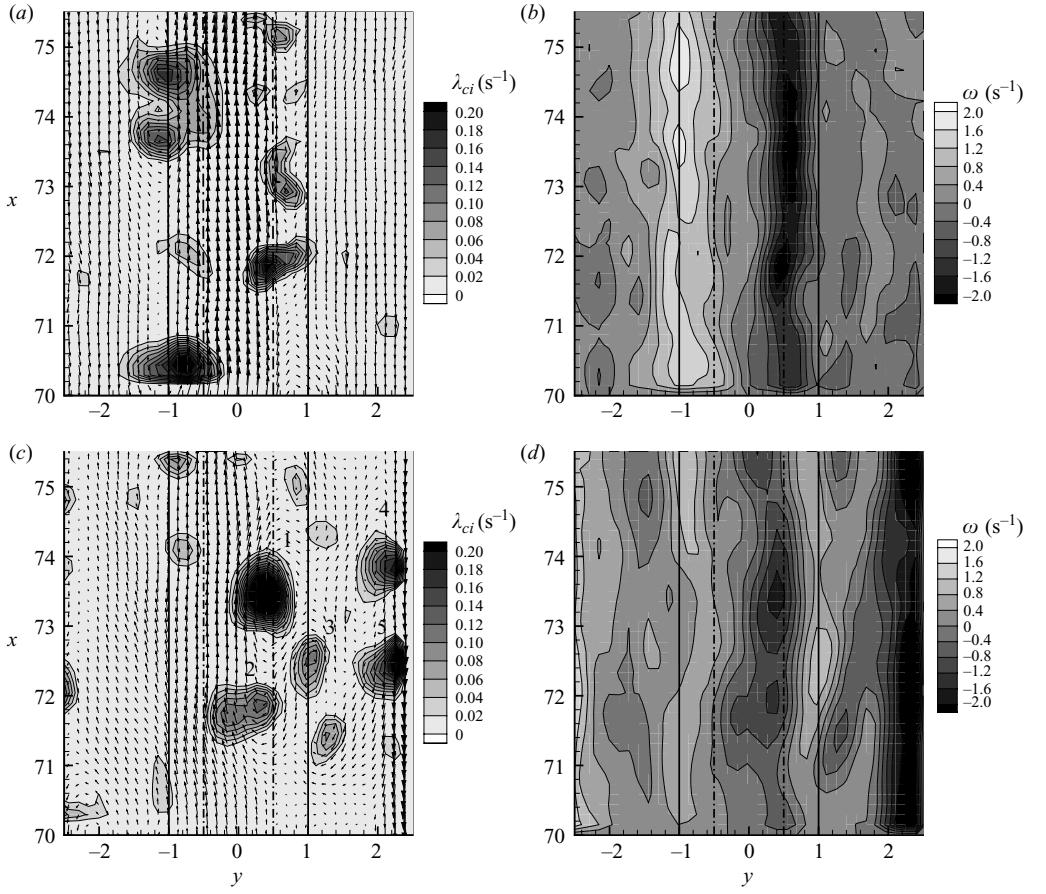

FIGURE 3. Velocity vector fields, after a Galilean decomposition, and swirling strength contour maps for 'shallow flows' (Q008) (*a*) and 'intermediate flows' (Q120) (*c*); (*b*) and (*d*): the corresponding vorticity fields.

are considered. In fact, in the case of 'shallow flows', inspection of figure 3(*a*, *b*) reveals that the transition regions are dominated by large-scale macro-vortices and the sense of rotation is positive (anticlockwise) for the left shear layer and negative (clockwise) for the right shear layer. The macro-vortices are aligned in the region with a spanwise distance in the range $(0.5\text{–}1)W^*_{mc,hw}$ from the main-channel axis, which corresponds to the region of high turbulence. The macro-vortices remain confined in the transition region and almost no macro-vortices are present above the floodplains. Their formation can be explained in terms of the vorticity generation mechanism at the depth jumps described in Soldini *et al.* (2004). Increasing the discharge leads to the 'intermediate flows' for which the surface velocity is characterized by slightly weaker double shear layers in the transition regions and strong wall shear layers above the floodplains; this can be seen in the vorticity distribution as well as in the vortex positions in figure 3(*c*, *d*). For example, vortices 1, 2 and 3 are located in the transition region, vortices 1 and 2 rotate clockwise while vortex 3 rotates anticlockwise. Vortices 4 and 5, both located in the wall shear layers, have negative vorticity and, therefore, rotate clockwise. Finally, for the 'deep flows', not shown in the figure, macro-vortices are observed only close to the sidewalls and none is present at the

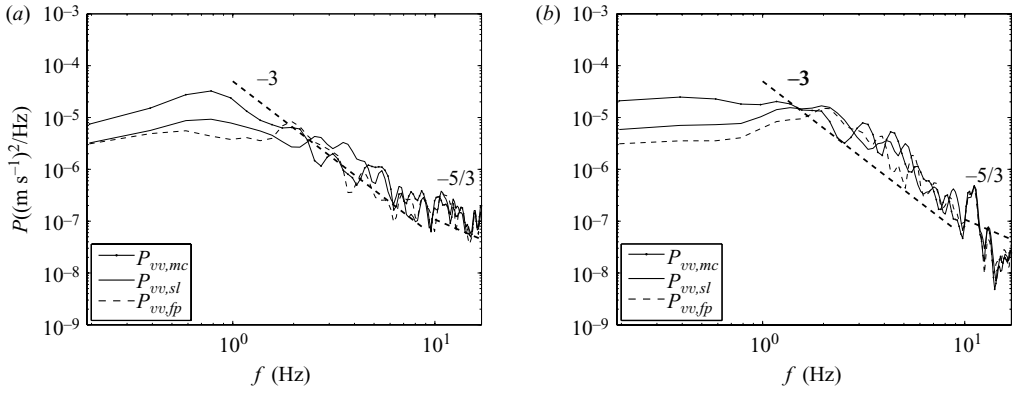

FIGURE 4. Power spectral density for cases Q018 and Q120.

transition region. In this case, the difference in the flow depth between the floodplains and the main channel is no longer an active mechanism to generate vorticity. For all the experiments, we have never observed vortex breaking and/or vortex merging. The macro-vortices once generated are convected downstream without interacting with each other. The width of the main channel is such that the vortices at the two transitional regions are always sufficiently distant. The background shearing of the mean flow is not so intense as to produce vortex breaking (Tabeling 2002).

PSD distributions of transverse velocity fluctuations for single point signals are plotted for both a shallow flow case Q018 (see figure 4*b*) and intermediate flow case Q120 (see figure 4*a*). Three spanwise positions were chosen for the analysis of the PSD distributions: the main channel (mc), the shear layer (sl) and the flood plain (fp). Both plots show a -3 regime for frequencies between 1 and 10 Hz, and for frequencies greater than 10 Hz the data is not inconsistent with a $-5/3$ regime. The low-frequency regime shows that the flow is dominated by large-scale quasi-two-dimensional macro-vortices, both for the 'shallow flows' and 'intermediate flows' (Jirka 2001; Tabeling 2002). The energy scalings found in the present context are consistent with the results discussed in Nikora *et al.* (2007) for the subcritical flow conditions. The range of the Froude number investigated does not cover the supercritical regime where a different scaling has been found in the general case of a free-surface flow (Nikora *et al.* 2007).

3.3. *The main properties of the macro-vortices*

In this section, we focus on the main features of the macro-vortices by a statistical analysis. It is first fundamental to characterize features of the eddies in dependence of their generation mechanism which, as above mentioned, is the depth jump in the transition region for 'shallow flows' and the flow shearing at the lateral walls for 'intermediate' and 'deep flows'. Macro-vortices of different sizes are generated depending on the flow depth ratio. To detail such dependencies we have analysed both the PDFs of the vortex area-equivalent radius (figure 5*a–d*) of both transition region vortices and wall vortices. For shallow flows ($r_h > 3$), vortices are found to reside mainly in the transition region and with typical size in the range $R_{eq} = 0.5{-}1$. For 'intermediate' and 'deep flows' macro-vortices both increase in size and frequency over the floodplains, whereas the transition regions exhibit a decreasing vortex content. The PDFs of the R_{eq} seem to suggests that floodplain vortices tend to be smaller than those generated at the transition region. A relevant result of the above analysis

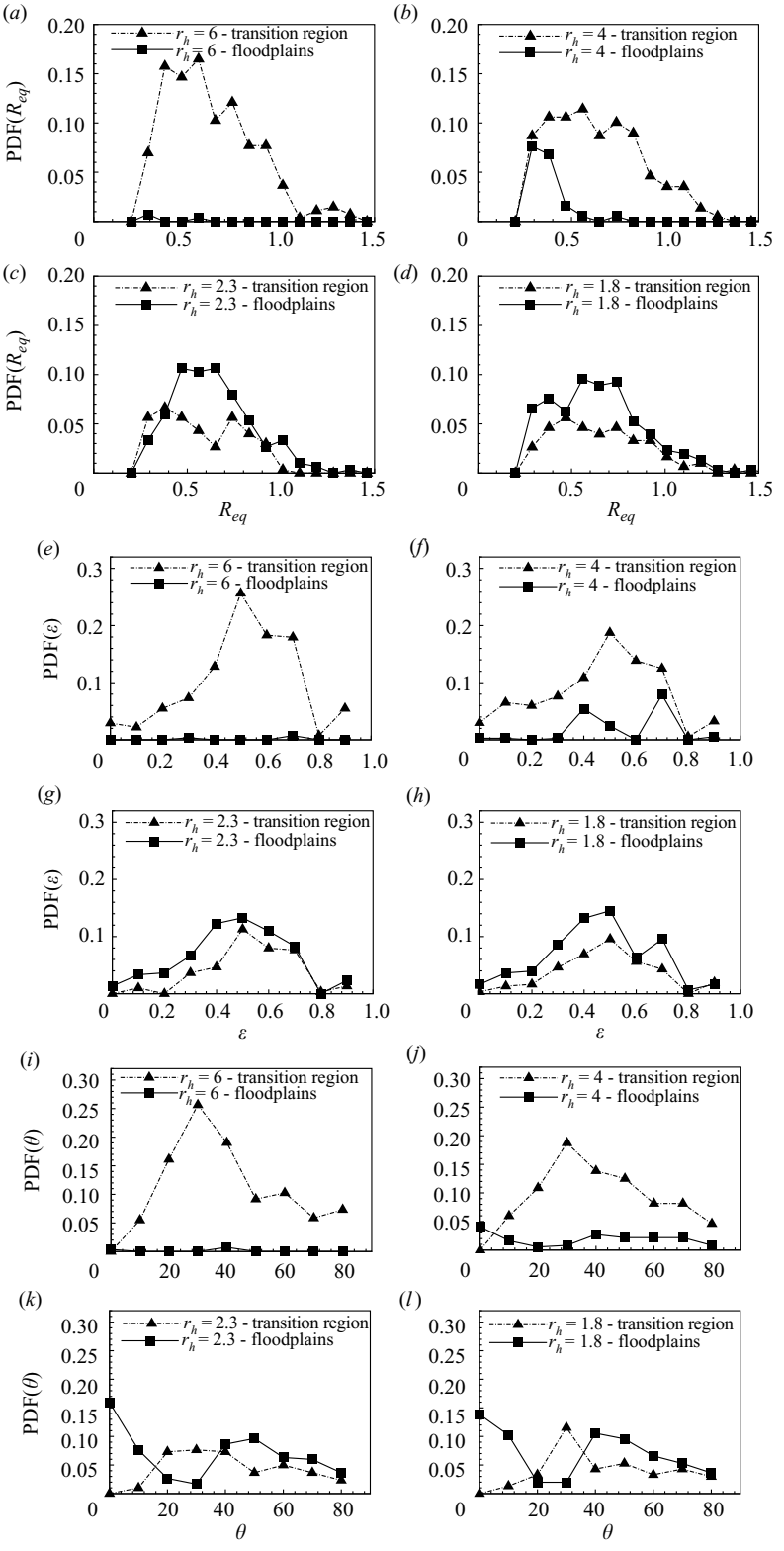

FIGURE 5. PDFs of macro-vortex size and shape: equivalent radius R_{eq}, vortex eccentricity ϵ and the alignment angle θ for different depth ratios.

is that R_{eq} of the transition vortices well compares with the width of the transition region itself, as observed numerically by Soldini *et al.* (2004).

Besides the distribution of the equivalent radius, we have analysed also the shape of the vortical structures observed either on the transitional regions or on the floodplains. In particular, we have computed the eccentricity ϵ, defined as the ratio between the major and minor axes of the vortex, which is a measure of the vortex symmetry ($\epsilon = 1$ represents a perfectly circular vortex). PDFs of ϵ are reported in figure 5(*e–h*). In the 'shallow flows' regime transitional macro-vortices are rather elongated with values of $\epsilon \approx 0.55$–0.60. For smaller ratios r_h, the vortices, which are more concentrated over the floodplains, are characterized by a similar distribution of eccentricity with a primary peak at $\epsilon \approx 0.5$ and a secondary maximum at $\epsilon \approx 0.7$ In the case of two-dimensional free turbulence, it has been found that elliptical vorticity patches are, in general, unstable. Due to the difference in rotation between the vortex core and the edges, elliptical vortices are subjected to filamentation and, ultimately, they tend to become circular. This process is known as 'axisymmetrization' (see Tabeling 2002, and cited references). In the present case, the latter process is likely to be inhibited by the topographic forcing and the resulting background shearing, causing the vortical structure to remain more elongated.

Finally, we have calculated the PDFs and mean values of the angle θ that expresses the orientation of the main axis of the vortex with respect to the mean flow (perfect vortex-mean flow alignment is achieved for $\theta = 0$) are shown in figure 5(*i–l*). For 'shallow flows' macro-vortices are observed to be oriented to the mean flow with an angle $\theta \approx 40^\circ$–50°. Decreasing r_h, the vortices, mainly concentrated along the lateral walls, are characterized by a bimodal distribution of orientation peaked at $\theta \approx 0^\circ$ and $\theta \approx 50^\circ$, whereas macro-vortices generated at the transition regions are characterized by a broader orientation distribution. This suggests that wall vortices are, on average, more aligned with the mean flow than those generated at the transition region. Moreover θ, independent of $\mathrm{d}u/\mathrm{d}y$ over the transition region and weakly decreasing over the floodplain, ranges, in average, between 20° and 50°. Thus, in general, macro-vortices are not parallel to the main flow and those covering the transition region are not sensitive to the mean shear (a decrease of θ with $\mathrm{d}u/\mathrm{d}y$ is expected for alignment due to shearing) and those over the floodplains are weakly aligned by the mean shear. As a consequence, the transition macro-vortices are likely to weakly engulf the floodplain fluid, more similarly to what happens for wakes than for jets/shear layers. In fact, the shear at the transition region of a jet is strong enough to align the interface vortices parallel to the mean interface; this does not happen for wakes (Mobbs 1968).

4. Discussion and conclusions

A detailed and extensive experimental investigation based on PIV analysis of free-surface velocities has been made to reveal the fundamental features of the flow characterizing a straight compound channel from the inception to fully developed conditions. Specific focus was on elucidating the properties of horizontal flow mixing and pointing out similarities/differences with a true free shear flow. In this respect, a first difference is made evident by the mean flow profile shown in figure 2(*a*). For most of the values of the depth ratio r_h, a non-monotonic profile characterizes the fully developed flow. Hence, bell-type function, typically used as self-similar solutions for free shear layers (Chu, Wu & Khayat 1991; van Prooijen & Uijttewaal 2002), is inadequate to represent the mean flow in a compound channel. Moreover, although

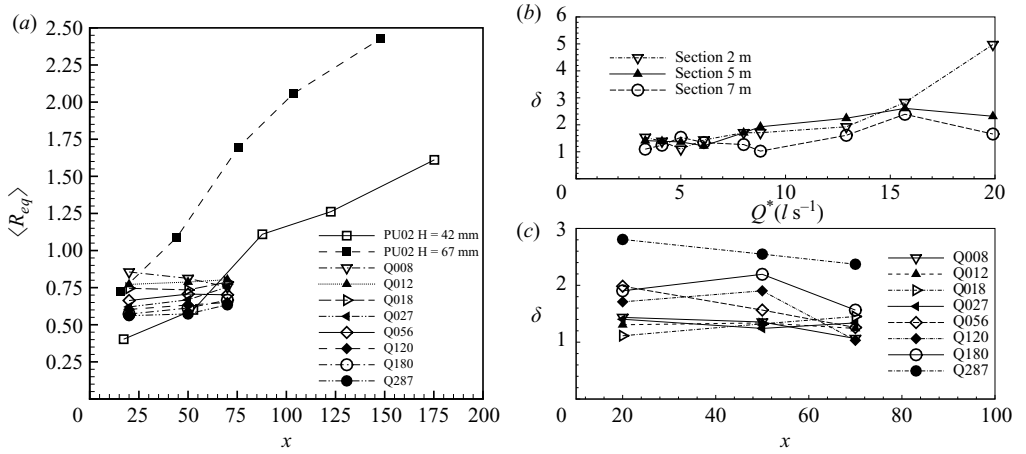

FIGURE 6. (*a*) Comparison of the mean equivalent radius $\langle R_{eq} \rangle$ versus normalized downstream distance between the present measurements and the experiments of van Prooijen & Uijttewaal (2002); dimensionless shear layer thickness δ as a function of both the dimensional discharge Q^* (*b*) and the dimensionless downstream distance x (*c*).

horizontal mixing is governed by the quasi-two-dimensional macro-vortices in both flows, differences are expected, because the vortical structures of the two flows seem to have rather different properties. Such a difference is easily appreciated by inspecting figure 6(*a*), which illustrates, in suitable dimensionless form, the downstream growth of the mean equivalent radius $\langle R_{eq} \rangle$, derived from the PDFs shown in the previous section, for the macro-vortices observed in the present experiments, and those measured in free shear flows by van Prooijen & Uijttewaal (2002). While the former ones have a size almost constant with x, the latter ones grow in size at a considerable rate. This is consistent with the fact that the thickness δ of a free shear layer is expected to grow linearly in the streamwise direction, whereas in the case of compound channels δ remains constant, as soon as the flow is fully developed (see figure 6*c*). The dependence of δ on the flow discharge is shown in figure 6(*b*). This is a reflection of the fundamental fact that the size of compound channel macro-vortices scales with the crossflow size of the transition region, which remains constant along x, (Soldini *et al.* 2004; Piattella, Brocchini & Mancinelli 2006) whereas shear-layer macro-vortices scale with the shear layer width that increases downstream of the inception (see figure 5 of van Prooijen & Uijttewaal 2002). Moreover, macro-vortices are also found to reside in different spatial regions in the two flows. In the case of a free shear layer the vortex position, coinciding with that of the shear layer, is seen to bend towards the low-velocity region of the shear layer (van Prooijen & Uijttewaal 2002). On the contrary, in a compound channel, not only the lateral walls provide an extra agent for vortex generation (mainly confined over the flood plains), but also transition-region macro-vortices are found to reside over the transition region only.

In conclusion, the main findings of the present study can be summarized as follows:

(*a*) The global dynamics of a straight compound channel cannot be entirely explained by a shear layer approach, i.e. the flow largely differs from that obtained by the meeting of three parallel streams of different velocity. The compound channel topography and sidewall boundaries force a non-monotonic velocity profile. Generation and evolution of macro-vortices in compound channel flows is seen to strongly depend on the depth ratio r_h (Soldini *et al.* 2004). The observed

macro-vortices have a size almost independent of the streamwise coordinate and that clearly scales with the crossflow extension of the transition region.

(*b*) The shape and the orientation of the transitional vortices suggest that engulfment of floodplain fluid by the main channel flow is more similar to that of a wake than that of a jet/shear layer.

The results here described will be used as the basis for a theoretical analysis that, in analogy to recent studies of other types of open channel flows (e.g. shallow wakes discussed in Negretti *et al.* 2006), will allow for an analytical description of the mean flow.

Thanks go to Dr A. C. Rummel for contributing to the early stages of this study. The two anonymous referees are thanked for their valuable comments and suggestions.

REFERENCES

Adrian, R. J., Christensen, K. T. & Liu, Z. C. 2000 Analysis and interpretation of istantaneous turbulent velocity fields. *Exp. Fluids* **29**, 275–290.

Bousmar, D., Proust, N., Riviereand, S., Paquier, A., Morel, R. & Zech, Y. 2005 Upstream discharge distribution in compound-channel flumes. *J. Hydraul. Engng ASCE* **131** (5), 1408–1413.

Chu, V. H., Wu, J. H. & Khayat, R. E. 1991 Stability of transverse shear flow in shallow open channels. *J. Hydr. Engng* **117** (10), 1370–1388.

Jirka, G. H. 2001 Large scale flow structures and mixing processes in shallow flows. *J. Hydraul. Res.* **39**, 567–573.

Mobbs, F. R. 1968 Spreading and contraction at flows. *J. Fluid Mech.* **33**, 227–240.

Negretti, M. E., Vignoli, G., Tubino, M. & Brocchini, M. 2006 On shallow-water wakes: an analytical study. *J. Fluid Mech.* **567**, 457–475.

Nezu, I., Onitsuka, K. & Iketani, K. 1999 Coherent horizontal vortices in compound open-channel flows. In *Hydraulic Modeling* (ed. V. P. Singh, I. W. Seo & J. H. Sonu), pp. 17–32. Water Resources Publication.

Nikora, V., Nokes, R., Veale, W., Davidson, M. & Jirka, G. H. 2007 Large-scale turbulent structure of uniform shallow free-surface flows. *Environ. Fluid Mech.* **7**, 159–172.

Piattella, A., Brocchini, M. & Mancinelli, A. 2006 Topographically-controlled, breaking wave-induced macrovortices. Part 3. The mixing features. *J. Fluid Mech.* **559**, 81–106.

van Prooijen, B. C., Battjes, J. A. & Uijttewaal, W. S. J. 2005 Momentum exchange in straight uniform compound channel flow. *J. Hydraul. Engng* **131** (3), 175–183.

van Prooijen, B. C. & Uijttewaal, W. S. J. 2002 A linear approach for the evolution of coherent structures in shallow mixing layers. *Phys. Fluids* **14** (12), 4105–4114.

Sellin, R. H. J. 1964 A laboratory investigation into the interaction between the flow in the channel of a river and that over its flood plain. *La Houille Blanche* **7**, 793–802.

Shiono, K. & Knight, D. W. 1991 Turbulent open-channel flows with variable depth across the channel. *J. Fluid Mech.* **222**, 617–646.

Socolofksy, S. A. & Jirka, G. H. 2004 Large-scale flow structures and stability in shallow flows. *J. Environ. Engng Sci.* **3**, 451–462.

Soldini, L., Piattella, A., Brocchini, M., Mancinelli, A. & Bernetti, R. 2004 Macrovortices-induced horizontal mixing in compound channels. *Ocean Dyn.* **54**, 333–339.

Stephenson, D. & Kolovopoulos, P. 1990 Effects of momentum transfer in compound channels. *J. Hydraul. Engng ASCE* **116**, 1512–1522.

Tabeling, P. 2002 Two-dimensional turbulence: a physicist approach. *Phys. Rep.* **362**, 1–62.